

The DIRECT Project: Influence of Blending on the Cepheid Distance Scale.

II. Cepheids in M33

B. J. Mochejska¹

Copernicus Astronomical Center, 00-716 Warszawa, Bartycka 18

e-mail: mochejsk@camk.edu.pl

L. M. Macri, D. D. Sasselov², K. Z. Stanek

Harvard-Smithsonian Center for Astrophysics, 60 Garden St., Cambridge, MA 02138

e-mail: lmacri, dsasselov, kstanek@cfa.harvard.edu

ABSTRACT

We investigate the influence of blending on the Cepheid distance scale. Blending is the close association of a Cepheid with one or more intrinsically luminous stars. High-resolution *HST* images are compared to our ground-based data, obtained as part of the DIRECT project, for a sample of 102 Cepheids in the M33 galaxy. The average (median) flux contribution from luminous companions not resolved on the ground-based images in the *B*, *V* and *I* bands (S_B , S_V , S_I) is about 29% (15%), 24% (14%), 30% (21%) of the flux of the Cepheid. For 64 Cepheids with periods in excess of 10 days the average (median) values of S_B , S_V , S_I are 20% (10%), 16% (7%), 23% (14%). This shows that, depending on the sample of objects chosen, the distance derived from our ground-based *V*-band magnitudes for the M33 Cepheids would be systematically underestimated by about 8%-11% (3%-6%).

Using artificial star tests we study crowding and blending as separate phenomena. These tests indicate that the effect of blending could be more significant than crowding in regions of lower surface brightness, below 21.6 mag/□". We also find indications that in the case of long period Cepheids ($P > 10^d$) companions from blending are on average bluer than companions introduced by crowding.

Our ground-based resolution in M33 corresponds to the *HST* resolution at about 11 Mpc. We estimate the effect of blending at resolutions corresponding to a range of distances as observed with the *HST* using the *HST* M33 data as the template unblended population. We compare our results to those obtained by other groups.

¹Visiting Student, Harvard-Smithsonian Center for Astrophysics

²Alfred P. Sloan Foundation Fellow

1. Introduction

As the number of extragalactic Cepheids discovered with *HST* continues to increase and the value of H_0 is sought from distances based on these variables (e.g. Saha et al. 1999; Freedman et al. 2001), it becomes even more important to understand various possible systematic errors which could affect the extragalactic distance scale. Currently, the most important systematic is a bias in the distance to the Large Magellanic Cloud, which provides the zero-point calibration for the Cepheid distance scale. The LMC distance is very likely significantly shorter than usually assumed (e.g. Udalski 2000; Stanek et al. 2000, Fitzpatrick et al. 2001). It still might be considered uncertain at the $\sim 10\%$ percent level (e.g. Jha et al. 1999). Another possible systematic, the metallicity dependence of the Cepheid Period-Luminosity (PL) relation, is also very much an open issue, with empirical determinations ranging from 0 to -0.4 mag dex $^{-1}$ (Freedman & Madore 1990; Sasselov et al. 1997; Kochanek 1997; Kennicutt et al. 1998).

In this paper we investigate the influence of blended stellar images on the derived Cepheid distances. We define *blending* as the close projected association of a Cepheid with one or more intrinsically luminous stars, which cannot be detected within the observed point-spread function (PSF) by photometric analysis (e.g., DAOPHOT, DoPHOT). Such blended stars are mostly other young stars which are physically associated – from actual binary and multiple systems to companions which are not gravitationally bound to the Cepheid. Blending is thus a phenomenon different from *crowding* or *confusion noise*; the latter occurs in stellar fields with a crowded and complex background due to the random superposition of stars with different luminosities. In this paper, we are concerned with blending due to wide systems.

The issue of the effect of blending on the derived Cepheid distances has received some attention since the appearance of our first paper on M31 Cepheids (Mochejska et al. 2000, hereafter Paper I). An estimate of the magnitude of this effect for remote galaxies was obtained by Stanek & Udalski (1999) using the LMC stellar population as the template. Their analysis indicated that blending could be a significant (up to 20%) source of systematic error in distances determined using Cepheids. Saha, Labhardt & Prosser (2000) studied the effect of confusion noise on Cepheid derived distances using artificial star tests. Their experiment showed that this effect is within 0.1 mag for NGC 4639 at a distance of 25 Mpc. A further study of the effects of crowding and confusion noise was conducted by Ferrarese et al. (2000) as part of the HST Key Project on the Extragalactic Distance Scale, employing artificial star tests. They estimated that the photometry of Cepheids could be biased too bright by up to 0.2 mag due to crowding. Under the assumption that multiple epoch data can be used to reject most of the affected Cepheids, they derived an upper limit of 0.02 mag for the bias in the distance scale due to crowding. Gibson, Maloney & Sakai (2000) presented three empirical tests of blending. Their results were inconclusive and only indicated at a 1σ level that blending for Cepheids located in the LMC bar is not representative for the distant galaxies observed by the HST Key Project. An uncertainty of ${}_{-0}^{+5}\%$ due to crowding and/or blending was included into the systematic error budget in the HST Key Project final results paper (Freedman et al. 2001). Macri et al. (2001a) studied the effect

of blending in an inner field of M101 by scaling to its distance the stellar populations observed with NICMOS in M31 and M81. They concluded that this effect could be significant and lead to a 0-0.2 mag bias in the derived distance modulus.

We investigate the effects of stellar blending on the Cepheid distance scale by studying two Local Group spiral galaxies, M31 and M33. The results for M31 were presented in Paper I. In this paper, second of the series, we concentrate on M33, which for the purposes of this paper we assume to be located at a distance of 850 kpc. As part of the DIRECT project (Kaluzny et al. 1998), we have collected an extensive data set for this galaxy, and thus far have discovered ~ 400 Cepheids, among other variables. We identify some of these Cepheids on archival *HST*-WFPC2 images and compare them to our ground-based data to estimate the impact of blending on our photometry, taking advantage of their superior resolution – the $0''.12$ FWHM on the WFPC2 camera (Ferrarese et al. 2000) corresponds to ~ 0.5 pc at the distance of M33, compared to ~ 6 pc for the ground-based data.

This paper is organized as follows: Section 2 describes the ground-based and *HST* data and the applied reduction procedures. In Section 3 we discuss the process of identifying Cepheids on *HST* WFPC2 images. In Section 4 we present the Cepheid blending catalog and discuss it in Section 5. In Section 6 we present the results of artificial star tests. In Section 7 we show an example of an extremely blended Cepheid. The implications of our results for remote galaxies are studied in Section 8. In Section 9 we discuss the results of other investigations of Cepheid blending and/or crowding. The concluding remarks are to be found in Section 10.

2. Observations and Data Reduction

2.1. Ground-based Data

The ground-based data were obtained as part of the DIRECT project between September 1996 and October 1997 during 42 nights on the F. L. Whipple Observatory 1.2 m telescope and 10 nights on the Michigan-Dartmouth-MIT 1.3 m telescope. Three $11' \times 11'$ fields A, B and C with a scale of $0.32''/\text{pixel}$ were monitored, located north, south and southwest of the center of M33, respectively. The data for fields A and B has been reduced and the *BVI* photometry of 251 Cepheid variables published by Macri et al. (2001b). The reduction of the field C data, which is now part of a larger field Y, is in progress and the results will be reported by Stanek et al. (2001). The applied reduction, calibration and variable selection procedures were described by Kaluzny et al. (1998).

2.2. HST data

The archival *HST*-WFPC2 data used in this paper were retrieved from the Hubble Data Archive. We selected images overlapping our M33 fields observed from the ground, taken in filters F439W, F450W (roughly *B*), F555W, F606W ($\sim V$) and F814W ($\sim I$). The pixel scales of the Wide Field (WF) and Planetary Camera (PC) chips are 0.1 and 0.046 "/pixel, respectively.

The HST data overlapping our fields A and B had already passed through the standard preliminary processing and calibration procedures prior to its placement in the Archive. The HST data for field C, retrieved later, was calibrated by the On-The-Fly Calibration (OTFC) system at the time when our request was processed. The standard pipeline calibration and the OTFC are fully described in the *HST* Data Handbook.

The images were corrected under IRAF³ for the geometric distortion in the WFPC2 optics and for bad pixels (Stetson 1998). Whenever possible, the images were combined to remove cosmic rays. The photometry was extracted using the DAOPHOT/ALLSTAR package (Stetson 1987, 1992). A more detailed description of the reduction procedure can be found in Paper I.

It should be noted that the *HST* photometry has not been calibrated to any standard system and therefore instrumental magnitudes are used throughout this paper. This has, however, no bearing on the results presented in this paper, since they are strictly based on differential photometry.

3. The Identification of DIRECT Cepheids in *HST* Data

The preliminary identification of DIRECT Cepheids on the *HST* frames was performed under SAOimage ds9⁴ by a visual comparison of the *HST* data matched via World Coordinate System (WCS) information to our ground-based *V*-band templates. The WCS information for the ground-based template image header was derived by matching stars from the image to the USNO A2.0 Catalog stars (Monet et al. 1996) using the WCSTools image astrometry toolkit (Mink 1999).

Our list of Cepheids consists of an early version of the Macri et al. (2001b) catalog supplemented by field C Cepheids with periods in excess of 10 days. We have matched a total of 102 Cepheids to *HST* data: 48 in field A, 39 in field B and 15 in field C. There are 64 Cepheids with periods over 10 days in this sample.

In some cases a Cepheid which appeared to be a single star on the *V*-band template was

³IRAF is distributed by the National Optical Astronomy Observatories, which are operated by the Association of Universities for Research in Astronomy, Inc., under cooperative agreement with the NSF.

⁴SAOimage ds9 was developed under a grant from NASA's Applied Information System Research Program (NAG5-3996), with support from the Chandra Science Center (NAS8-39073)

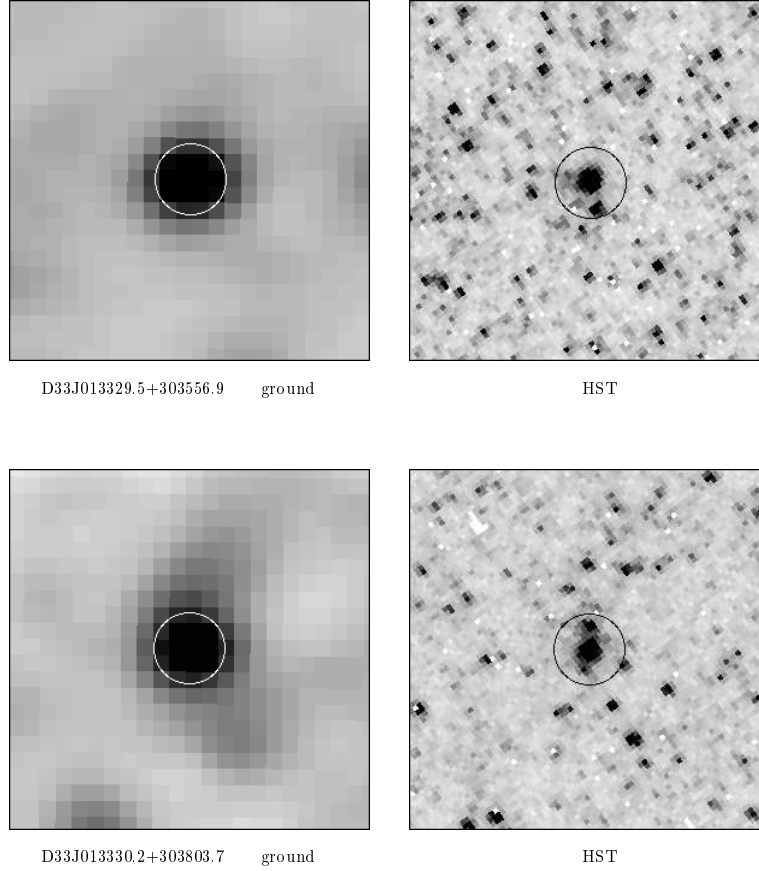


Fig. 1.— A comparison of the ground-based and *HST* images of two Cepheids: D33J013329.5+303556.9 and D33J013330.2+303803.7. Circles $0''.75$ in radius are drawn centered on the Cepheids.

resolved into multiple stars on an *HST* image. Two examples are shown in Figure 1. The images plotted in the left panels are from the *V*-band template image (FWHM $\sim 1''.4$) and those in the right panel were taken with the WF chips of the WFPC2 camera. Circles $0''.75$ in radius are drawn centered on the Cepheids. The Cepheid D33J013329.5+303556.9 is shown in the upper panels. On the ground-based template it appears as a single star, while on the *HST* image it is resolved into two objects differing by 2.5 magnitudes in brightness. The lower panels show the case of D33J013330.2+303803.7, where the Cepheid, single on the ground *V*-band template, is resolved by *HST* into three stars, with the two companions fainter by 2 and 3 magnitudes.

To help confirm the Cepheid nature of the objects selected, instrumental color-magnitude diagrams (CMDs) were constructed from *HST* data, whenever photometry in two bands was available. A few representative $(v_{F555W}, v_{F555W} - i_{F814W})$ CMDs are shown in Figure 2. The Cepheids are denoted by circles and their companions by squares. Stars from the same image are plotted in the background for reference. The upper panels present two Cepheids with blue blends (those shown in Fig. 1). D33J013329.5+303556.9, in the upper left panel, has a blue companion

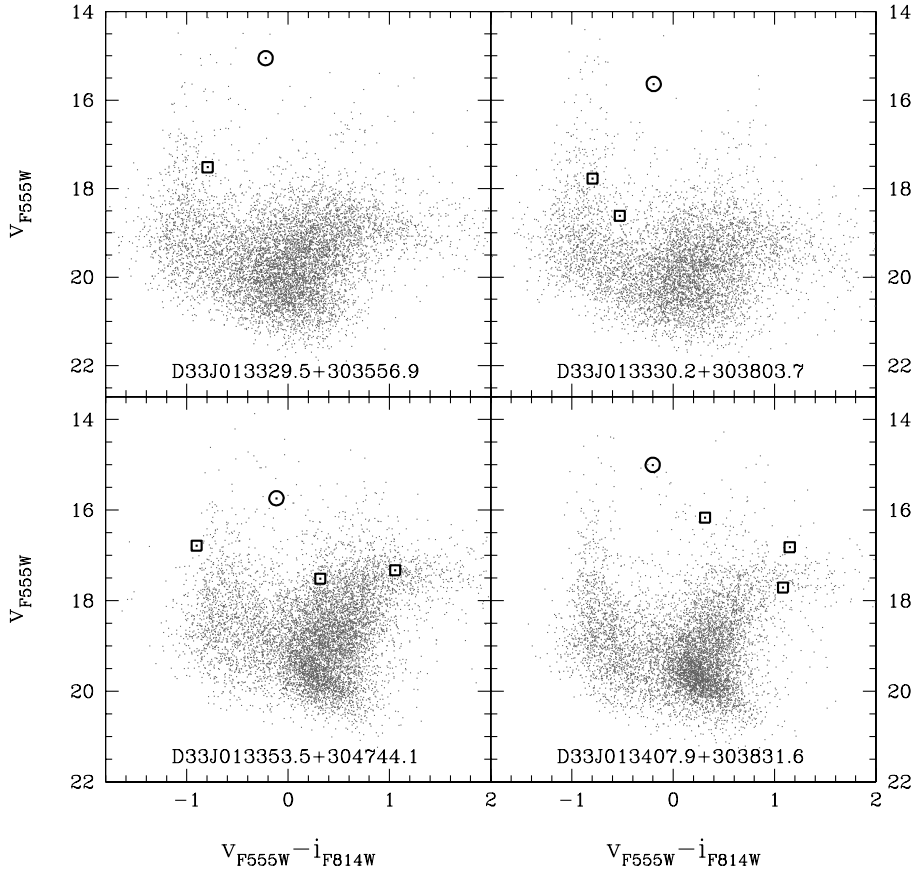


Fig. 2.— Selected $(v_{F555W}, v_{F555W} - i_{F814W})$ instrumental color-magnitude diagrams for Cepheids and their companions within $0''.75$ based on *HST* data. The Cepheids are denoted by circles and their companions by squares. Stars from the same image are plotted in the background.

contributing 10% of its flux in V and 6% in I . D33J013330.2+303803.7, in the upper right panel, has two blue blends at the level of 14% and 6% in V and 8% and 5% in I . In the lower left panel we show the Cepheid D33J013353.5+304744.1 with one blue and two red companions at the level of 33%, 24%, 20% in V and 18%, 64%, 29% in I . D33J013407.9+303831.6 in the lower right panel is a case with three red blends at the level of 34%, 19%, 8% in V and 55%, 10%, 27% in I .

3.1. The extremely blended Cepheid D33J013341.3+303212.7

In our ground-based M33 data we have discovered a highly blended Cepheid, exhibiting a very low amplitude of variability and the color of an upper main sequence star (D33J013341.3+303212.7, $P = 20.15^d$). We present this Cepheid as more of a curiosity or an instructive example than a problem in the determination of distances. Such Cepheids can be very easily rejected on the basis of their low amplitudes and often discrepant colors.

Without the a priori knowledge of the degree of contamination by blending, we have estimated

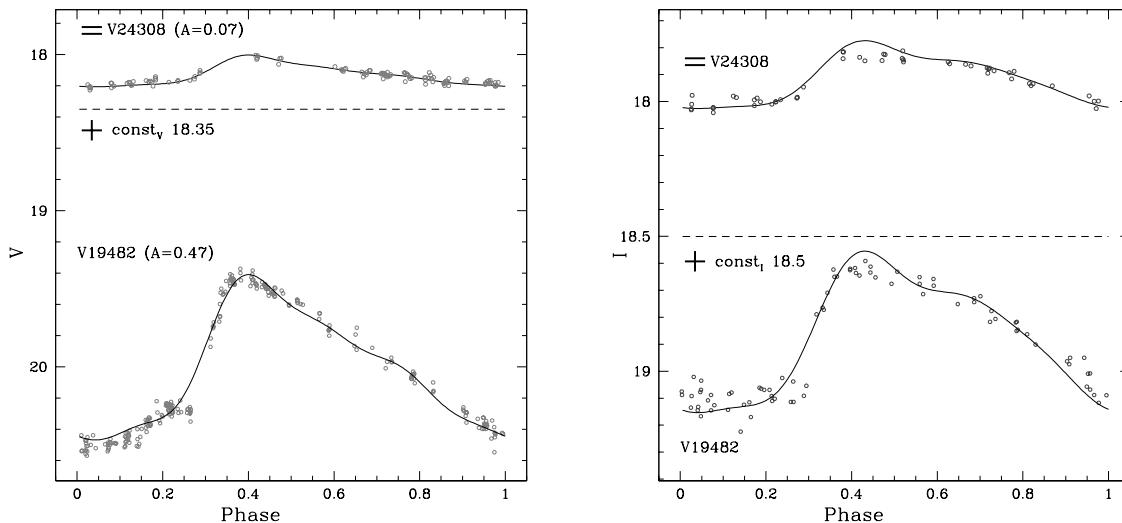


Fig. 3.— A comparison of the VI light curves of the extremely blended Cepheid D33J013341.3+303212.7 (V24308) and the unblended Cepheid D33J013324.7+303517.2 (V19482) with a similar period.

the brightness of the companion in V and I by adding constant flux to the VI light curves of a Cepheid with a very similar period ($P = 20.51^d$, $V = 19.96$, $V - I = 1.10$), to achieve the best match with the light curve of the highly blended Cepheid (Fig. 3). From the above analysis we have obtained a V magnitude of 18.35 mag and $V - I$ color of -0.15 mag for the blend.

An investigation of this variable in the HST data yielded the values of $S_V = 3.10$ and $S_B = 6.60$. Taking into account the phase at which the Cepheid was at the time of the HST observation, the blending companion is brighter by 1.53 mag than the Cepheid in the V -band. In B this difference amounts to about 2 mag. The 1.53 mag difference in V agrees very well with the 1.61 mag derived from light curve analysis.

4. The M33 Blending Catalog

We have adopted three criteria that a companion to a Cepheid has to fulfill to be included into our catalog as a blend. The star has to:

1. be located at a distance less than $0''.75$ from the Cepheid,
2. be undetected by DAOPHOT in our ground-based images,
3. contribute at least 6% of the flux of the Cepheid in the same filter.

The choice of maximum distance was motivated by the typical full width at half maximum (FWHM) in our ground-based images ($\sim 1''.5$). We have increased the minimum flux of the blend from 4% of the flux of the Cepheid, as adopted in our study of blending in M31 (Paper I) to 6%, to obtain a little more conservative estimate.

We have examined the Cepheids on the *HST* images to check for false detections (cosmic rays in case of single images, bad columns, etc.) or companions missing from the DAOPHOT list. In the former case the object was removed from the photometry list, in the latter its coordinates were entered by hand and DAOPHOT was run again on the corrected list.

To quantify blending we have used the parameter S_F , defined in Paper I as the sum of all flux contributions in filter F normalized to the flux of the Cepheid:

$$S_F = \sum_{i=1}^{N_F} \frac{f_i}{f_C} \quad (1)$$

where f_i is the flux of the i -th companion, f_C the flux of the Cepheid on the *HST* image and N_F the total number of companions.

We have also determined the surface brightness around the Cepheids on the ground-based V -band images taken on the same night as the photometric standards. The surface brightness was computed as the mode within a 20 pixel radius. We used a bin width of 1 ADU for the histogram to compute the value of the mode, smoothed with a flat-topped rectangular kernel (boxcar) filter 11 units in length. After correcting for the sky level, the instrumental surface brightness values were converted to mag/\square'' using 7-8 fairly bright isolated reference stars with known standard magnitudes. The *rms* scatter around the value of the average ranged from 0.042 to 0.071 mag/\square'' .

In Table 1 we present the blending catalog for 102 Cepheids found on the *HST* images: the name, the period, the mean V , I and B magnitudes taken from Macri et al. (2001b) and Stanek et al. (2001), the number of companions N_F and their total flux contribution S_F in the V , I and B bands respectively. The V , as in N_V and S_V , refers to filters F555W and F606W, I to F814W and B to F439W and F450W. For Cepheids identified on more than one *HST* image, the average values of S_F are listed. The last column gives the V band surface brightness Σ_V within a 20 pixel ($6''.4$) radius.

5. Discussion of the Properties of Blending

5.1. The Magnitude of the Effect of Blending

In Table 2 we present blending statistics for the M33 Cepheids. We list the average and median blending in BVI filters for the entire sample and for two subsamples, consisting of the Cepheids with periods below and above 10 days, respectively. The sizes of the samples (N) are also given. For all three samples blending is most significant in the I -band (21% all P, 29% $P < 10^d$,

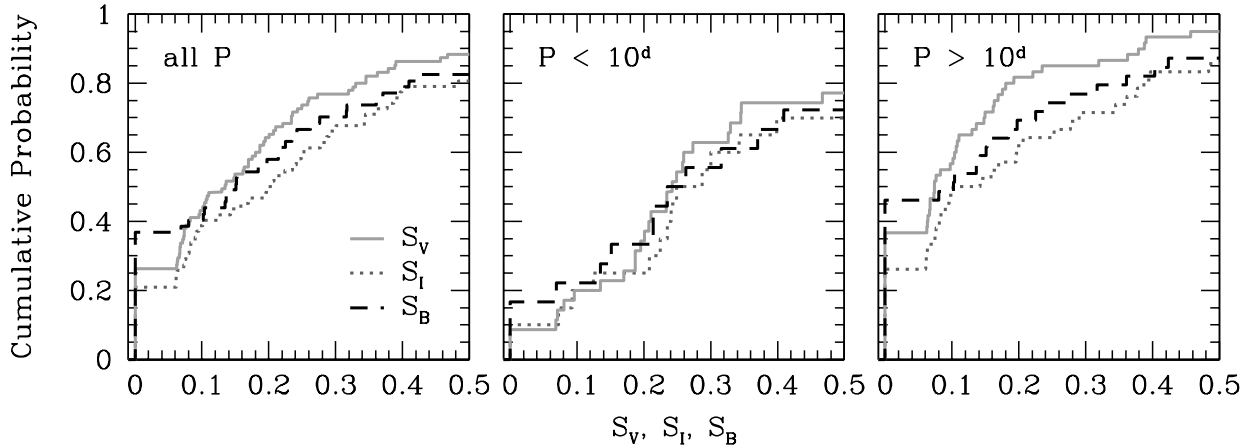


Fig. 4.— The cumulative probability distributions of S_V , S_I and S_B for M33 Cepheids (the continuous, dotted and dashed lines, respectively). The panels, going from left to right, show the distribution for the entire sample, for Cepheids with periods below and above 10 days, respectively.

14% $P > 10^d$), intermediate in B (15%, 26%, 10%) and least in V (14%, 25%, 7%). Blending is more substantial for the short period Cepheids.

Figure 4 shows the cumulative probability distributions of S_V , S_I and S_B for the M33 Cepheids, using solid, dotted and dashed lines, respectively. The panels, going from left to right, show these distributions for the entire sample and for Cepheids with periods below and above 10 days, respectively. The plots are restricted to Cepheids with blending S_F up to 0.5, to show in more detail the most interesting range, where cases with blending cannot be easily distinguished and rejected. About 80-90% of all Cepheids are contained within this range.

As expected from the Period-Luminosity relation, the short period (hence fainter) Cepheids suffer more from blending than do the long period (hence brighter) ones. Upon examining Fig. 4, we again note that the contribution from blends tends to be strongest in the I -band, intermediate in B and weakest in V . This trend is best seen in the long period sample. A likely explanation can be found by examining the CMDs in Fig. 2. Our limit of $S_F = 6\%$ corresponds to a difference of 3.05 magnitudes in brightness between the Cepheid and its companion. The stars which could

Table 2. THE M33 CEPHEID BLENDING STATISTICS

Period range	S_V			S_I			S_B		
	<i>avg</i>	<i>med</i>	<i>N</i>	<i>avg</i>	<i>med</i>	<i>N</i>	<i>avg</i>	<i>med</i>	<i>N</i>
all Periods	0.24	0.14	95	0.30	0.21	62	0.29	0.15	57
P < 10 days	0.37	0.25	35	0.43	0.29	20	0.47	0.26	18
P > 10 days	0.16	0.07	60	0.23	0.14	42	0.20	0.10	39

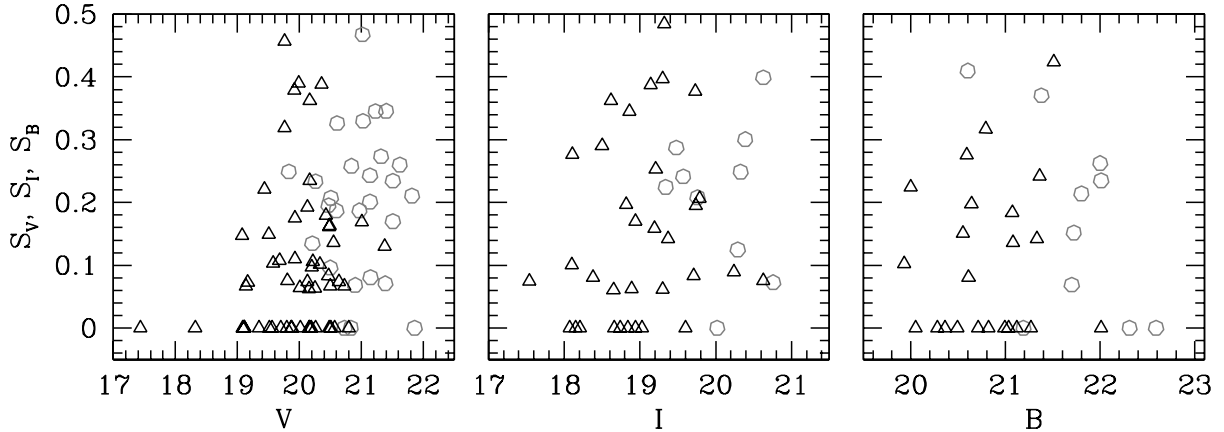


Fig. 5.— The blending parameters S_V , S_I and S_B as functions of the respective ground-based standard mean magnitudes. Short period Cepheids are indicated with circles, long period ones with triangles.

contribute enough flux to become blends will thus most likely be located on the upper main sequence (MS) or on the red giant branch (RGB). In effect there should be more companions which are brightest in the B -band (upper MS) or in I (RGB) and relatively few in V .

In case of the short period Cepheids, below $S_F = 0.25$ ($\sim 50\%$ of the sample) blending is equal across all bands. Two factors could account for this behavior: poorer statistics due to the smaller size of the sample, especially in B and I , and the increased contribution of faint intermediate color blends. Above $S_F = 0.25$, V -band seems to be least affected by blending.

Another feature seen in this Figure is the relatively large number of unblended Cepheids in the B band, compared to I and, especially, V . This might be due to the fact that on average the *HST* exposure times in V and I were 2 – 3 times longer than in B . The fainter blends in B could thus elude detection, especially in case of the short period Cepheids.

In Figure 5 we show the blending parameters S_V , S_I and S_B as functions of the respective ground-based standard mean magnitudes. Short period Cepheids are indicated with circles and long period ones with triangles. No clear correlation of blending with the magnitude of the Cepheid is seen, although the short period Cepheids appear on average to be more blended, in accordance with Fig. 4. There is a substantial overlap in brightness for the short and long period samples.

5.2. The Colors of the Blends

In Figure 6 we present the relative color distributions of the blends in $S_I - S_V$ (top) and $S_V - S_B$ (bottom). The panels, going from left to right, show these distributions for the entire sample and for Cepheids with periods below and above 10 days, respectively. Only Cepheids with

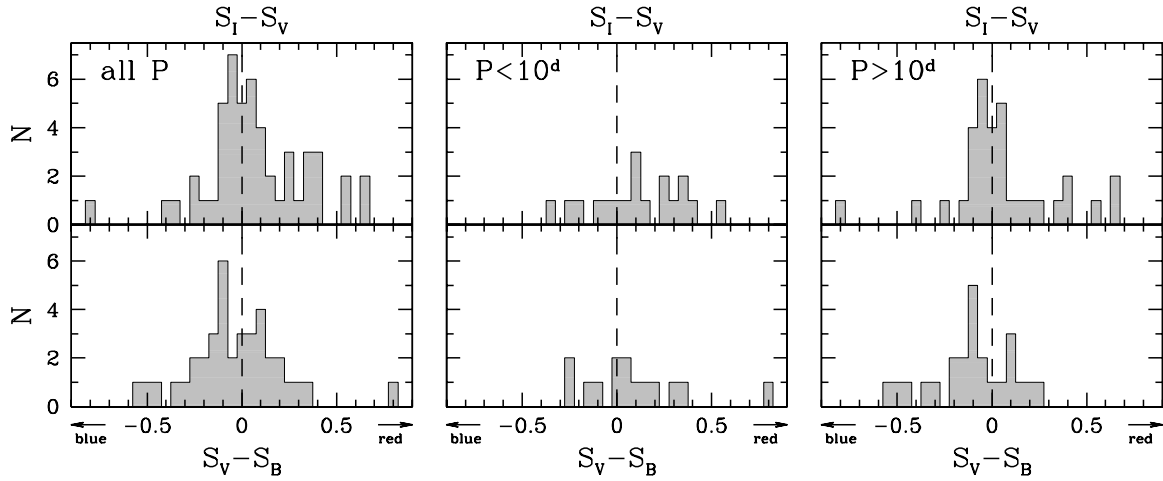


Fig. 6.— The relative color distributions of the blends in $S_I - S_V$ (top) and $S_V - S_B$ (bottom). The panels, going from left to right, show the distribution for the entire sample and for Cepheids with periods below and above 10 days, respectively.

non-zero blending in at least one of the bands are plotted. Table 3 lists the median colors and the number of cases of red and blue blending for each of the three period ranges.

The color distributions of the blends for the entire Cepheid sample exhibit maxima approximately at 0. The maxima show double peaks due to the fact that most blends are either redder or bluer than the Cepheids. In the $S_V - S_B$ distribution there are almost as many red blends as there are blue, while in $S_I - S_V$ there is a noticeable excess of red blends.

After decomposing the sample into long and short period Cepheids it becomes apparent that the sample of short period Cepheid blends is markedly the redder of the two. This is at least in part due to the correlation between Cepheid luminosity and color – fainter Cepheids are bluer than brighter ones. For the long period Cepheids blue blends dominate in $S_V - S_B$, where there are twice as many blue blends as red. The $S_I - S_V$ color distribution is almost uniform. The peak is shifted slightly to the blue, but a red tail is present. The double structure of the maxima is more prominent than in the entire sample, especially in $S_V - S_B$.

Table 3. THE M33 CEPHEID BLEND COLOR STATISTICS

Period range	$S_I - S_V$			$S_V - S_B$		
	<i>med</i>	N_{red}	N_{blue}	<i>med</i>	N_{red}	N_{blue}
all Periods	0.05	31	20	-0.02	17	21
P < 10 days	0.10	13	5	0.08	9	5
P > 10 days	0.02	18	15	-0.09	8	16

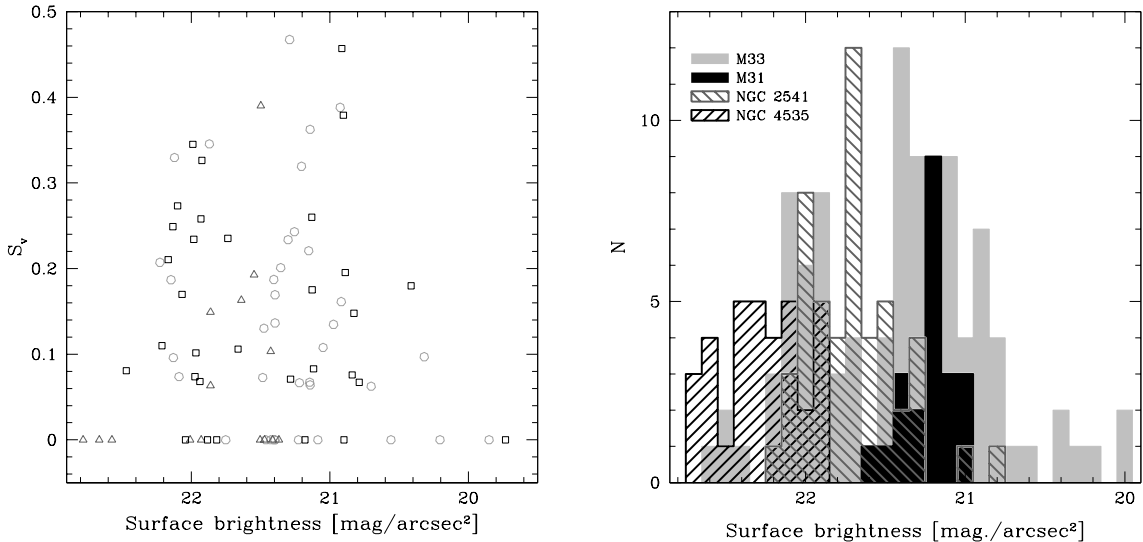


Fig. 7.— Left panel: Blending S_V as a function of the surface brightness within a radius of $6''.4$ around the M33 Cepheids on the ground-based images. Field A Cepheids are denoted by squares, field B by circles and field C by triangles. Cepheid blending does not seem to correlate with surface brightness. Right panel: The surface brightness around Cepheids in M33, M31, NGC 4535 and NGC 2541.

5.3. The Environments of the Cepheids

There have been suggestions in the literature (e.g. Ferrarese et al. 2000) that blending should increase with the measured values of surface brightness. We investigate empirically this effect using our M33 data. The left panel of Figure 7 shows blending S_V as a function of the V -band surface brightness within a radius of $6''.4$ around the M33 Cepheids on the ground-based images. Field A Cepheids are denoted by squares, field B by circles and field C by triangles. We find no such correlation between blending and the underlying surface brightness – Cepheids in environments of different surface brightness show roughly the same frequency and amount of blending.

To put these values into perspective, we have computed the surface brightness for two galaxies which straddle their range, NGC 4535 and NGC 2541. The *HST* data for these galaxies, observed as part of the HST Key Project on the Extragalactic Distance Scale (Macri et al. 1999, Ferrarese et al. 1998), were obtained from the Hubble Data Archive. The implemented procedure was described in Paper I. In the right panel of Figure 7 we plot the surface brightness distributions for Cepheids in M33, M31 (Paper I), NGC 4535 and NGC 2541. As seen in the diagram, M33 spans a wide range in surface brightness – three magnitudes, from 19.7 to 22.8 mag/ \square'' . The distribution shows two clear maxima: the brighter one corresponds to Cepheids located within the spiral arms and the fainter one to those in regions in between the arms. There is also a tail of Cepheids from very bright regions, in the proximity of the M33 nucleus. M31 overlaps mostly

with the brighter maximum of M33. The NGC 4535 distribution peaks slightly above the fainter maximum of M33. NGC 2541 also overlaps the fainter maximum in M33, though about half of its Cepheids are located in regions of lower surface brightness, where our M33 coverage is much more sparse (4 Cepheids). We conclude that our Cepheids in M33 reside in environments of surface brightness typical of spiral galaxies.

6. Crowding vs. Blending - Artificial Star Tests

In our previous paper on blending of Cepheids in M31 (Paper I) we have made a distinction between the phenomena of crowding and blending. We defined *blending* as the close projected association of a Cepheid with one or more intrinsically luminous stars, mostly other young stars which are physically associated - from actual binary and multiple systems to companions which are not gravitationally bound to the Cepheid. In the case of our investigation we are limited by resolution to wide systems. *Crowding* or *confusion noise* occurs in stellar fields with a crowded and complex background due to the random superposition of stars of different luminosity.

In such dense fields as are observed in galaxies, the blending estimate for a Cepheid will also include crowding. Based on our M33 data we will try to address the issue of the importance of blending relative to crowding. If we assume that a Cepheid is associated with other luminous stars located in its proximity, then moving it to a randomly chosen position on the image will break that association. In the former case, the Cepheid will be subject to blending; in the latter, to crowding.

To estimate the influence of crowding we have generated a catalog of randomly distributed stars with the same magnitudes as the actual Cepheids, following the same technique as for the Cepheid blending catalog. For each Cepheid observed on a WFPC2 image we generated a list of 100 random positions and determined the contribution from companions at that location. We also determined the surface brightness values on the ground-based images around these positions. Our artificial star catalog, thereafter referred to as the *artificial* catalog, contains data for ~ 9200 realizations in V , ~ 5300 in I and ~ 3000 in B .

The construction of the blending catalog described in Section 4 (thereafter referred to as *corrected*) involved the visual examination of all putative companions, to correct for missing and/or false detections. The large number of realizations in the artificial crowding catalog precluded us from making a similar inspection. Therefore, the original unaltered catalog of Cepheid blends (thereafter *uncorrected*) seems to be the more natural choice for a comparison between blending and crowding. In the discussion that follows, we have used the uncorrected blend catalog; K-S tests show that at confidence levels of 93%-100% the distributions for the corrected and uncorrected catalogs are consistent with a single distribution (Tab. 4).

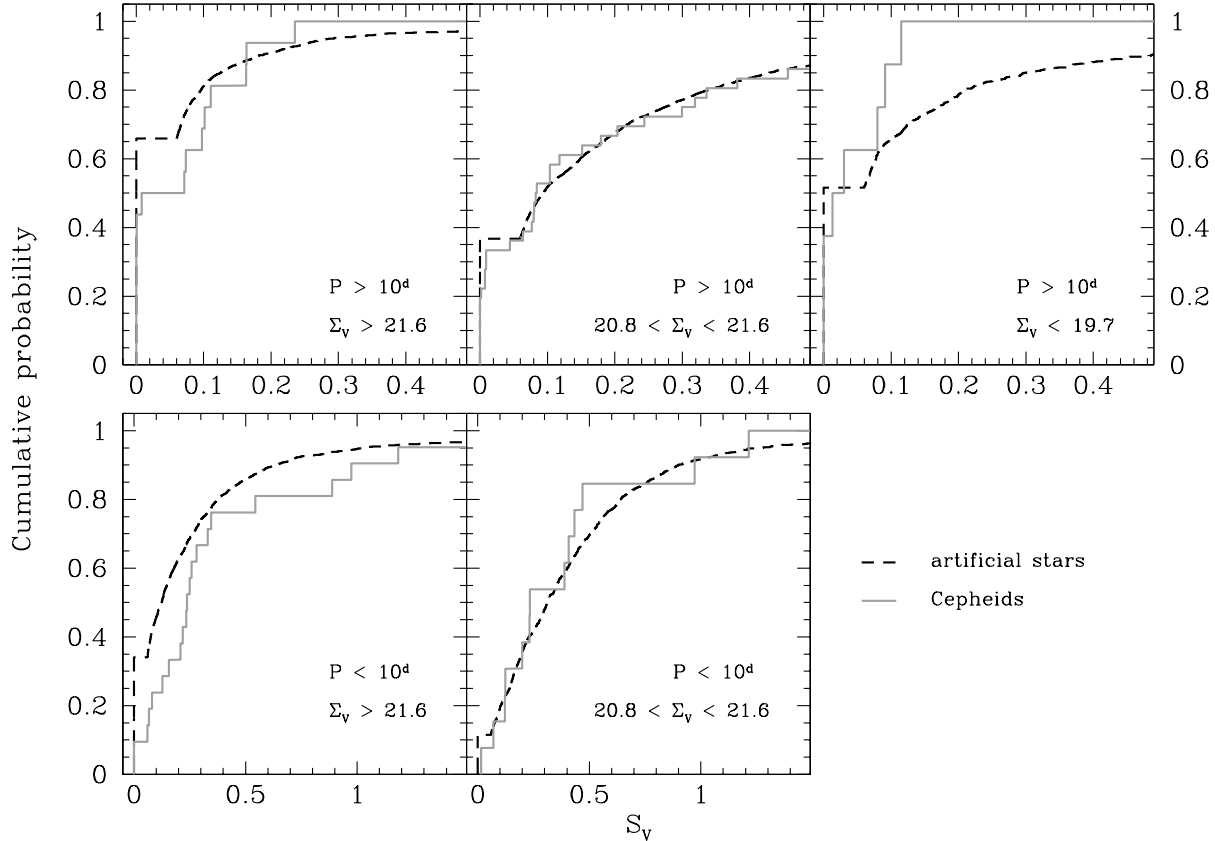


Fig. 8.— The cumulative probability distributions of the blending parameter S_V for the artificial Cepheids (dashed line) and the uncorrected Cepheid catalog (solid).

6.1. The Magnitude of the Effects of Blending and Crowding

We have divided the sample of M33 Cepheids into two bins in period at $P = 10^d$ and three bins in surface brightness, separated at $\Sigma_V = 21.6$ and $\Sigma_V = 20.8$ mag/ \square'' . The division into different surface brightness regions was motivated by the clear separation of Cepheids located inside and outside the spiral arms and the existence of a high surface brightness tail associated with the nucleus, as seen in the right panel of Fig. 7. The magnitude of the effect of crowding will be different in each of the three ranges of surface brightness, therefore we have decided to analyze them separately.

Figure 8 shows the cumulative probability distributions for S_V drawn from the artificial crowding catalog (dashed line) and the uncorrected Cepheid blending catalog (solid line). We show the distributions for Cepheids with $P > 10^d$ in the upper panels and with $P < 10^d$ in the lower ones. Note that the scales on the S_V axes are different for the two period ranges. The left, middle and right panels show the lowest, medium and highest surface brightness regions, respectively. The lower right panel is not drawn, as there was only one short period Cepheid in the highest surface brightness range.

Let us first consider the Cepheids located in regions of lowest surface brightness (leftmost panels of Fig. 8). A visual inspection reveals that blending is stronger than crowding for these Cepheids. The K-S test confirms the impression that these data sets are different, giving a 1% and 3% probability that they are drawn from the same distribution, for the short and long period Cepheids, respectively. The difference between the magnitude of those two effects for the long period Cepheids is not as large as for the short period ones. This is expected, as a short period (fainter) Cepheid will yield a higher value of S_V than a long period (brighter) Cepheid when blended with a star of the same magnitude.

We now move on to Cepheids located in intermediate surface brightness regions (middle panels of Fig. 8). At first glance, it appears that the magnitude of the effects of blending and crowding is comparable. For the short period Cepheids the K-S test shows that these data sets are consistent with a single distribution at a confidence level of 93%. In case of the long period sample, the K-S test gives a probability of only 10%. Nevertheless, even if the distributions differ, the two effects are still similar in magnitude.

Finally, we examine the case of Cepheids located in the highest surface brightness regions (upper right panel of Fig. 8). We note that blending is weaker than crowding for these Cepheids. This effect is most likely due to selection effects. In regions of such high surface brightness we are biased towards finding luminous Cepheids with weaker than average blending. The K-S test results are not conclusive in determining whether or not these two data sets are drawn from different distributions. Also, crowding for these Cepheids is weaker than for those in the intermediate surface brightness regions, as luminous Cepheids are less susceptible to crowding.

The above analysis indicates that the importance of blending relative to crowding very likely increases with decreasing surface brightness. This is not unexpected, as young stars are known to cluster (Harris & Zaritsky 1999). Increasing the level of crowding will tend to obscure this effect.

6.2. The Colors of Blending and Crowding Companions

Figure 9 presents the relative color distributions of the blending and crowding companions in $S_I - S_V$ (top) and $S_V - S_B$ (bottom), drawn from the artificial star crowding catalog (hatched histogram) and the corrected Cepheid blending catalog (filled histogram). We only plot the distribution from the corrected catalog, since it is closer to the true color distribution than the one drawn from the uncorrected catalog. The panels, going from left to right, show the distribution for Cepheids with periods below and above 10 days, respectively. Only Cepheids with non-zero blending in at least one of the bands are plotted. The distributions are normalized to unity. The number of Cepheids from the corrected and uncorrected catalogs may be different, as some Cepheids will pass the 6% threshold in one catalog and not in the other.

Let us first examine the colors of the crowding companions. The $S_I - S_V$ color distributions are shifted towards the red, though the one for long period Cepheids is asymmetric, with a small

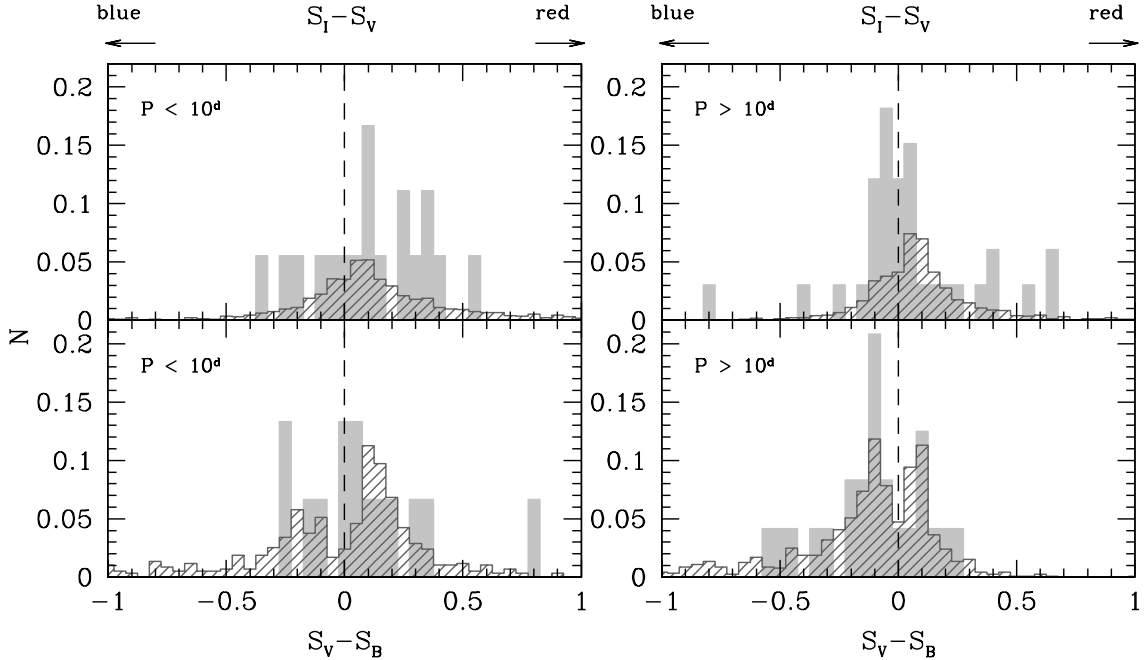


Fig. 9.— The relative color distributions of the blending and crowding companions in $S_I - S_V$ (top) and $S_V - S_B$ (bottom), drawn from the artificial crowding catalog (hatched histogram) and the corrected Cepheid blending catalog (filled histogram). The panels, going from left to right, show the distribution for Cepheids with periods below and above 10 days, respectively. The distributions are normalized to unity.

bump on the blue side. In $S_V - S_B$ the distributions show two peaks. For short period Cepheids the red peak is more pronounced, while for long period Cepheids they are comparable and there is a tail extending bluewards. This is consistent with the interpretation presented in §5.1. The stars which could contribute enough flux to cross the 6% threshold will most likely be blue stars on the upper MS or red stars on the RGB.

As far as can be inferred from the modest sample of short period Cepheids, the blends to the Cepheids show qualitatively similar color distributions as the companions due to crowding. The color distributions of long period Cepheid blends show subtle differences from the crowding color distributions. The $S_I - S_V$ color distribution of blends with long period Cepheids peaks to the blue of the distribution of crowding companions, while in $S_V - S_B$ the blue peak is more distinct than the red one, while for the artificial stars the two peaks were of comparable magnitude.

The above comparison indicates that the distribution of the colors of blends to the short period Cepheids and of crowding stars are most likely similar, while the blends to the long period Cepheids tend to be bluer than the crowding stars. If so, this would lend support to the notion that more luminous (hence younger) Cepheids should be located close to their place of formation, near other young blue stars.

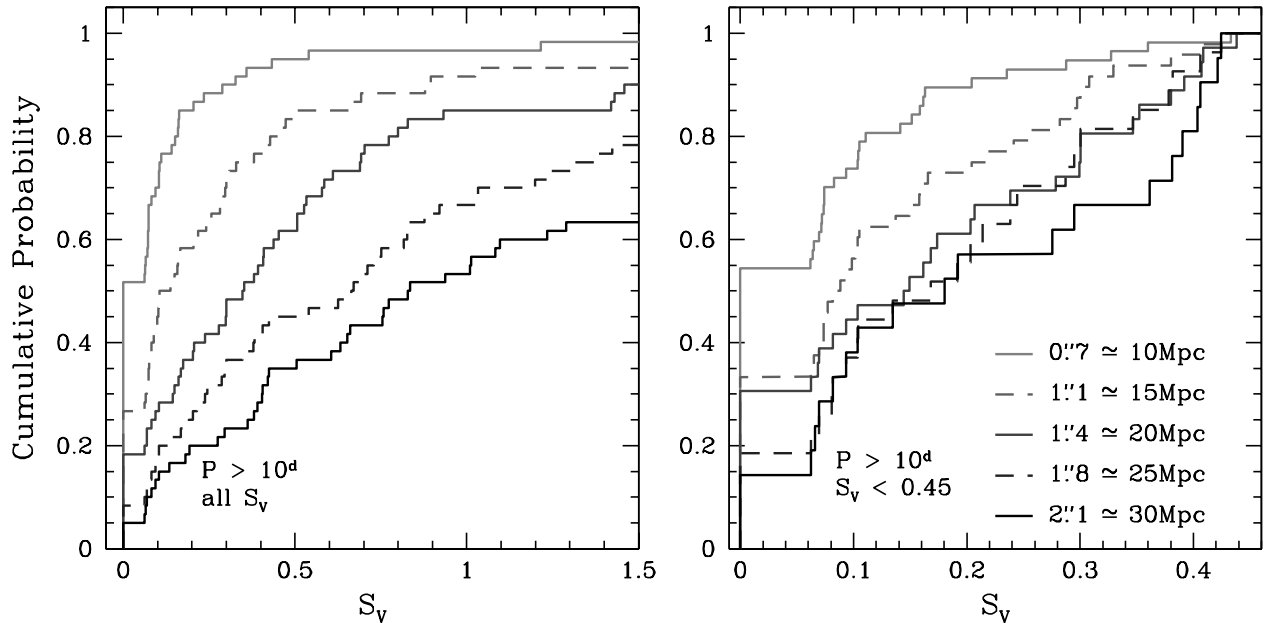


Fig. 10.— The cumulative probability distributions of blending parameter S_V for the M33 Cepheids within radii of $0''.7$, $1''.1$, $1''.4$, $1''.8$, $2''.1$, corresponding to $0''.12$ resolution at distances of 10, 15, 20, 25 and 30 Mpc, assuming a distance of 850 kpc to M33.

7. Indications for Remote Galaxies

As the number of extragalactic Cepheids discovered with *HST* continues to increase, it becomes crucial to obtain constraints on the bias in their photometry introduced by the effect of blending. Using the *HST* M33 data as the template we will try to obtain an estimate of the effect that blending would have on this galaxy if it were observed at their distances. The actual magnitude of the effect of blending will depend on many factors, such as the morphology of the host galaxy, the surface brightness of the regions in which the Cepheids are located, the brightness distribution of the Cepheids, the actual sample of Cepheids, the methods of variable extraction and classification, etc. Nonetheless, M33 can yield a useful order of magnitude constraint, as it is a spiral galaxy of surface brightness typical for those where Cepheids are sought and is observed at a moderate inclination (56° , Schmidt, Priebe & Boller 1993).

The average FWHM on the DIRECT project ground-based images of M33 is about $1''.5$, or ~ 6 pc. A similar spatial resolution would be achieved with the WF chips of the *HST*-WFPC2 camera for a galaxy at a distance of 11 Mpc. By increasing the radius around the Cepheid for summing the contributions of the blends we can simulate the deterioration of resolution due to the increasing distance to the galaxy. For our purpose we have chosen the radii of $0''.7$, $1''.1$, $1''.4$, $1''.8$, $2''.1$, corresponding to the $0''.12$ FWHM on the WF chips at distances of 10, 15, 20, 25 and 30 Mpc, assuming a distance of 850 kpc to M33. We have restricted ourselves to the long period ($P > 10^d$) sample, as long period Cepheids are preferred for determining distances.

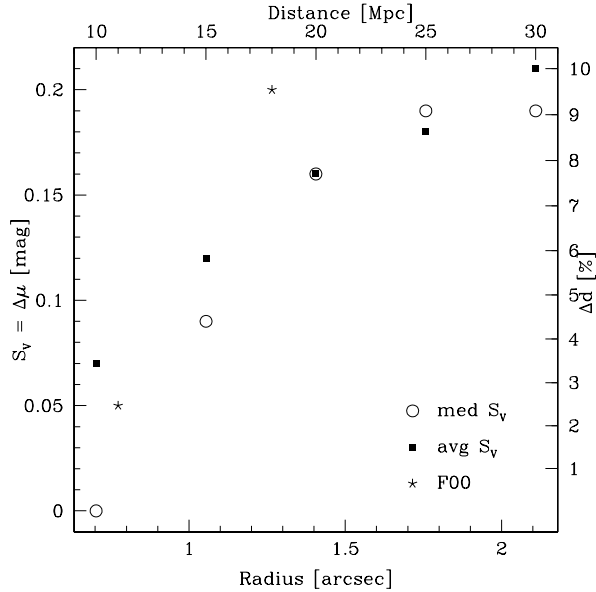


Fig. 11.— Blending/distance bias as a function of the summing radius/distance. The average and median S_V are indicated with open and filled symbols, respectively. The Ferrarese et al. (2000) results are indicated with asterisks.

The left panel of Figure 10 shows the cumulative probability distribution of S_V for different cutoff radii (proxy for distance). As expected, blending increases with distance and becomes severe at radii corresponding to M33 seen at distances of 20, 25 and 30 Mpc, where the median 0 of S_V are 37%, 68% and 89%. The highly blended Cepheids will of course be recognized as such based on the diminished amplitude of variability and, possibly, different colors.

In a study of crowding Ferrarese et al. (2000) find that it is virtually impossible to recognize a Cepheid with $S_V \leq 30\%$ as affected from the change in the amplitude of the light curve, and it only becomes possible for most Cepheids when S_V exceeds 60%. To make our estimate of blending more realistic we have redrawn these distributions in the right panel of Fig. 10 making the assumption that all Cepheids with $S_V > 45\%$ will be recognized as blended and rejected from the sample. Here blending also increases with distance for the most part, though the distributions are seen to cross each other on several occasions. Most striking is the case of the 25 Mpc and 30 Mpc distributions, where strong blending ($S_V > 20\%$) is more severe at 25 Mpc than at 30 Mpc. This is due to the fact that as the overall value of blending increases, the slope of the S_V distribution flattens out and does not change considerably in the relevant range of S_V .

The bias in distance due to blending is illustrated in Fig. 11 as a function of distance. At distances of 10-20 Mpc the bias increases from 0% – 3% to 8%, depending on the statistic used and levels off at 9% – 10% at 25-30 Mpc. The bias introduced by blending into the distance modulus expressed in magnitudes is to a very good approximation equal to S_V for $S_V \leq 0.2$.

8. Other investigations of blending

Since the appearance of our first paper based on M31 Cepheids (Paper I) the effect of blending on the Cepheid distance scale has been subject to further study. In this section we will present a short discussion of the results obtained by other groups and try to relate our results to theirs. In several papers our results and those of Stanek & Udalski (1999) discussed below, have been questioned; we will also address this issue.

Stanek & Udalski (1999) estimated the effect of blending for remote galaxies using the OGLE LMC Cepheid and star catalogs (Udalski et al. 1999, 2000) as the unblended template. Their approach involved summing the contribution of blends within a range of radii around the Cepheids, corresponding to the resolution of the WF camera at different distances. The distance moduli were derived from fitting the P-L relations to all Cepheids whose *I*-band amplitudes exceeded 0.4 mag after accounting for blending. Their results indicated that blending could introduce a substantial bias into Cepheid derived distances: <0.1 mag at distances <15 Mpc and 0.2-0.3 mag for more remote galaxies.

An analysis of the effect of confusion noise on Cepheid distances based on artificial star tests was presented by Saha, Labhardt & Prosser (2000). That work dealt with the contribution from the underlying confusion pattern resulting from the unresolved stellar background. Their simulations showed that this effect is within 0.1 mag for NGC 4639 at a distance of 25 Mpc. Our estimates include both confusion noise and stars that would be resolved if they were observed at a larger separation from the Cepheid. Therefore it is not surprising that the Saha et al. result is somewhat lower than our estimate of a 0.2 mag bias at a distance of 25 Mpc.

A further study of the effects of crowding and confusion noise, addressing specifically the case of the HST Key Project, was performed by Ferrarese et al. (2000) using artificial star tests. They estimated that the effect of crowding could bias the photometry of the Cepheids to be too bright by 0.05 mag for NGC 2541 at 11 Mpc and 0.2 mag for NGC 1365 at 18 Mpc.

The Ferrarese et al. simulations account only for the effect of crowding, and not for blending, which appears to be more significant than crowding in low surface brightness regions (Fig. 8). This dependence will most likely result from the clustering of Cepheids with other young stars and will become more prominent at lower levels of crowding. Such clustering has been observed for blue MS stars in the LMC (Harris & Zaritsky 1999).

Ferrarese et al. assume that most of the affected Cepheids can be rejected using multiple epoch data on the basis of several criteria, thus diminishing the bias in distance to less than 0.02 mag. One of these criteria is based on the assumption that affected stars should have larger photometric errors. We have investigated the existence of a correlation between Cepheid blending and the reported DAOPHOT/ALLSTAR photometric errors. In Figure 12 we plot the photometric errors of stars in M33 fields A and B as a function of magnitude, from Macri et al. (2001c). Cepheids are indicated by solid dots surrounded by circles of size proportional to their value of

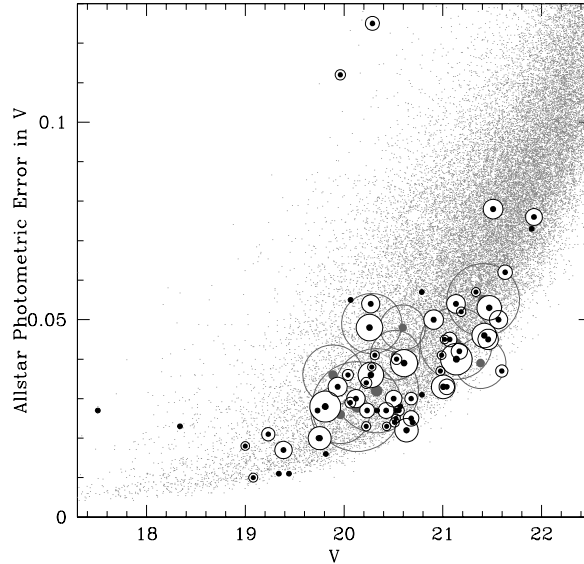


Fig. 12.— The Allstar photometric errors for the M33 field A and B stars as a function of the standard V -band magnitude. The Cepheids are indicated by solid dots surrounded by circles proportional in size to S_V (no outside circle means $S_V = 0$). The white-filled symbols indicate Cepheids with $S_V < 0.5$

S_V . The white-filled symbols indicate Cepheids with $S_V < 0.5$. This figure clearly illustrates that there is no correlation between photometric errors and S_V – any kind of cut based on photometric errors will not discriminate between affected and unaffected Cepheids.

Another selection criterion examined by Ferrarese et al. (2000) is that a Cepheid to be used in the distance determination should fall within the magnitude range applicable to its period range. In practice this amounts to the rejection of outliers deviating from the mean by more than 3 times the σ of the best fit (Ferrarese et al. 1998). In case of NGC 2541 at 12 Mpc the 3σ deviation corresponds to ± 0.81 mag in V and ± 0.54 mag in I . Even seriously affected Cepheids can pass this criterion. Ferrarese et al. (2000) confirm that it is virtually impossible to discriminate against Cepheids for which the contamination amounts to 30% or less of the Cepheid mean flux. These are the most common types of blends, and thus of greatest concern (only 15% of our $P > 10^d$ Cepheids have $S_V > 30\%$). Furthermore, they find that only when the contamination is increased above 60% are they able to recognize most Cepheids as affected.

We do not observe the correlation between blending and surface brightness, predicted by Ferrarese et al. (Fig. 6 in Paper I; Fig. 7). Contrary to their unsupported claim the M31 Cepheids used in our analysis are not located in regions where the stellar background is significantly brighter than for the HST KP galaxies (Fig. 7 in Paper I; Fig. 7). Lastly, based on the residuals from the H -band Tully-Fisher relation Ferrarese et al. concluded that the blending hypothesis could be ruled out at the 1.85σ level. As Gibson et al. (2000) pointed out, this result is erroneous, as they had neglected the uncertainties associated with each of the residuals.

Three empirical tests of blending were presented by Gibson, Maloney & Sakai (2000). The predicted influence of blending on Cepheid derived distances was quantified by fitting a functional form to the results for LMC Cepheids presented by Stanek & Udalski (1999), which, as indicated therein, seems to have on average higher surface brightness than a typical HST Key Project galaxy. The authors find that the observed distribution of peak luminosities for five type Ia SNe excludes the blending hypothesis defined as above at a $\sim 1 \sigma$ level. The second test, I and H -band Tully-Fisher residuals, is not able to discriminate between the no blending and strong blending hypothesis: both models differ from the best fit lines, at most, at the 1σ level. The third test involves the comparison of distance moduli derived separately from the PC chip and the WF chips. As the PC chip has twice the resolution of the WF chips, there should be a systematic difference between these distance moduli. For five galaxies at a distance of ~ 31 mag, the observed differences have an rms scatter of 0.08 mag around the mean value of 0.03 mag, while the predicted offset is 0.11 mag. We would advise caution when drawing conclusions from this comparison. There are many other factors that the authors have neglected which will invalidate the results of such a comparison, like poor statistics on the PC chips (9, 6, 6, 6 and 4 Cepheids for the five galaxies), different orientations of the camera with respect to the galaxy, selection effects (see upper right panel of Fig. 8), finite intrinsic width of the P-L relation. Gibson et al. results are inconclusive and only indicate at a 1σ level that blending for Cepheids located in the LMC bar is not representative for the distant galaxies observed by the HST Key Project.

The final HST Key Project paper (Freedman et al. 2001) includes into the systematic error budget an uncertainty of ${}_{-0}^{+5}\%$ due to crowding and blending. The authors conclude that to assess quantitatively the impact of unresolved blending effects would require simulations based on the distribution of Cepheids in a galaxy field unaffected by blending, such as the study applied to the M101 Cepheids observed with NICMOS (Macri et al. 2001a).

The choice of M101 as the target to study the effects of blending was motivated by the large differences in the H and J -band Cepheid-based distance moduli in the inner and outer M101 fields: $\Delta\mu_H = 0.46 \pm 0.12$ mag and $\Delta\mu_J = 0.37 \pm 0.12$ mag. The approach adopted by Macri et al. (2001a) involved scaling the stellar separations in the well resolved fields in M31 and M81 to the distance of M101 and their magnitudes to the exposure time of the M101 images. Artificial fields were generated from these star lists and Cepheid photometry extracted following the same procedure as for the actual data. The resulting distance moduli obtained from the Cepheid PL fits were found to be smaller than the input ones by 0-0.2 mag, depending on the applied period cutoff. Based on these results the authors conclude that a substantial fraction of the difference in the distance moduli could be due to blending. In addition, the fact that the inner M101 field Cepheids exhibit the same correlation between $\langle E(V - I) \rangle$ and $\langle E(V - H) \rangle$ as those in other galaxies suggests that on average, the contamination due to blending has not introduced a significant change in the color of the Cepheids.

The issue of blending has also been studied for stars in general, to estimate its influence on the shape of the derived luminosity functions. At high enough levels of stellar density an

individual resolution element may contain random clumps of several stars, and a photometric reduction package will not be able to recognize the multiple nature of the object. Renzini (1998) explored this issue on theoretical grounds and found that the number of blends is proportional to the square of both the surface brightness and the actual resolution. He concluded that meaningful photometry can be obtained for stars much brighter than the total luminosity observed in one resolution element. This effect was also investigated empirically by DePoy et al. (1993), who compared the luminosity functions derived from images binned by varying factors and by Stephens et al. (2001), using simulations of entire star clusters, as observed in M31 with NICMOS. Both groups find that due to extreme crowding, the measured luminosity function may appear to extend to brighter magnitudes than the true luminosity function. They also point out that typical artificial star experiments will not reproduce the effect of crowding discussed above.

9. Conclusions

We have determined the effect of blending in *BVI* for a sample of 102 Cepheids in the M33 galaxy by comparing our ground-based images collected with a 1.2 m telescope to archival *HST* data. We found the average (median) flux contribution from luminous companions not resolved on the ground-based images in the *V*, *I*, *B* bands (S_V , S_I , S_B) to be about 24% (14%), 30% (21%), 29% (15%) of the flux of the Cepheid. For 64 Cepheids with periods in excess of 10 days the average (median) values of S_V , S_I , S_B are 16% (7%), 23% (14%), 20% (10%). Blending is least significant in *V*, intermediate in *B* and strongest in *I*. These results show that depending on the sample of Cepheids chosen, our ground-based *V*-band photometry for the M33 Cepheids could be systematically underestimated by 8%-11% (3%-6%).

We have studied crowding and blending as separate phenomena using artificial star tests. Our results indicate that the effect of blending could be more significant than crowding in regions of lower surface brightness, below $21.6 \text{ mag}/\square''$. The two effects are comparable in magnitude in intermediate surface brightness regions ($20.8 \leq \Sigma_V \leq 21.6 \text{ mag}/\square''$).

We have also investigated the colors of the blends and of the crowding companions. The blends to short period Cepheids ($P < 10^d$) are on average redder than the blends to long period Cepheids ($P > 10^d$), in accordance with the Cepheid period–luminosity–color relation. In most cases, blending does not significantly influence the color of the Cepheid. As in the case of the blends, the crowding companions to short period Cepheids are on average redder than the companions to long period Cepheids. We compare the blending and crowding color distributions and find indications that for long period Cepheids the blends could on average be bluer than the companions introduced by crowding.

We have estimated the effect of blending at resolutions corresponding to a range of distances from 10 to 30 Mpc, using the *HST* M33 data as an unblended template stellar population. Assuming that all Cepheids with $S_V > 45\%$ will be recognized as blended and rejected from the

sample, we find that the distance underestimate increases from 0% – 3% to 8% at 10-15 Mpc and levels off at 9%-10% at 25-30 Mpc. This indicates that blending could potentially be a substantial source of error in the Cepheid distance scale.

As the result of blending with other unresolved stars, the Cepheids appear brighter than they really are when observed in distant galaxies with *HST*. As we compare them with mostly unblended LMC Cepheids, this leads to systematically low distances to galaxies observed with *HST*, and therefore to systematically high estimates of H_0 . The sign of the effect of blending on H_0 is opposite to that caused by the lower LMC distance (e.g. Udalski 2000; Stanek et al. 2000) and might be of comparable value, as discussed in this paper. It should be stressed that blending is a factor which contributes in only one direction, and therefore it will not average out when a large sample of galaxies is considered.

A potential solution to the problem of blending could be the Cepheid period - flux amplitude relation. Unfortunately this relation is not universal, as Paczyński & Pindor (2000) find that SMC Cepheids have lower amplitudes than those in the LMC and in our Galaxy. They suggest metallicity as the most natural reason for this difference. If this is the case and the metallicity dependence could be calibrated, the Cepheid period - flux amplitude relation could offer the possibility to obtain Cepheid distance determinations not affected by blending.

Janusz Kaluzny and Bohdan Paczyński have provided us with helpful comments on the manuscript. We would like to thank Janusz Kaluzny for providing us with his database management codes, Peter Stetson for the *HST* WFPC2 point-spread functions and Doug Mink for assistance in automating image astrometry. This work was partially based on observations with the NASA/ESA Hubble Space Telescope, obtained from the data Archive at the Space Telescope Science Institute, which is operated by the Association of Universities for Research in Astronomy, Inc. under NASA contract No. NAS5-26555. Support for this work was provided by NASA through Grant AR-08741 from the Space Telescope Science Institute. BJM was supported by the Foundation for Polish Science stipend for young scientists and the Polish KBN grants 2P03D003.17 to Janusz Kaluzny and 2P03D025.19. DDS acknowledges support from the Alfred P. Sloan Foundation. Partial support for KZS was provided by NASA through Hubble Fellowship Grant HF-01124.01-A from the Space Telescope Science Institute.

REFERENCES

- DePoy, D. L., Terndrup, D. M., Frogel, J. A., Atwood, B., Blum, R. 1993, *AJ*, 105, 2121
Ferrarese, L. et al. 1998, *ApJ*, 507, 655
Ferrarese, L. et al. 2000, *PASP*, 112, 177
Fitzpatrick, E .L., Ribas, I., Guinan, E. F., DeWarf, L. E., Maloney F. P., Massa, D. 2001, *ApJ*,
accepted (astro-ph/0010526)

- Freedman, W. L., & Madore, B. F. 1990, *ApJ*, 365, 186
- Freedman, W. L., et al. 2001, preprint (astro-ph/0012376)
- Gibson, B. K., Maloney, P. R., Sakai, S. 2000, *ApJ*, 530, L5
- Harris, J., & Zaritsky, D. 1999, *AJ*, 117, 2831
- Jha, S., et al. 1999, *ApJS*, 125, 73
- Kaluzny, J., Stanek, K. Z., Krockenberger, M., Sasselov, D. D., Tonry, J. L., & Mateo, M. 1998, *AJ*, 115, 1016
- Kennicutt, R. C., et al. 1998, *ApJ*, 498, 181
- Kochanek, C. S. 1997, *ApJ*, 491, 13
- Macri, L. M., et al. 1999, *ApJ*, 521, 155
- Macri, L. M., et al. 2001a, *ApJ*, 549, 721
- Macri, L. M., Stanek, K. Z., Sasselov, D. D., Krockenberger, M., Kaluzny, J. 2001b, *AJ*, 121, 870
- Macri, L. M., Stanek, K. Z., Sasselov, D. D., Krockenberger, M., Kaluzny, J. 2001c, *AJ*, 121, 861
- Mink, D. J. 1999, in *ASP Conf. Ser. 172, Astronomical Data Analysis Software and Systems VIII*, eds. D. M. Mehringer, R. L. Plante & D. A. Roberts (San Francisco: ASP), 498
- Mochejska, B. J., Macri, L. M., Sasselov, D. D., & Stanek, K. Z. 2000, *AJ*, 120, 810 (Paper I)
- Monet, D., et al. 1996, *USNO-SA2.0*, (U.S. Naval Observatory, Washington DC)
- Paczyński, B. & Pindor, B. 2000, *ApJ*, 533, L103
- Renzini, A. 1998, *AJ*, 115, 2459
- Saha, A., Labhardt, L., Prosser, C. 2000, *PASP*, 112, 163
- Saha, A., Sandage, A., Tammann, G. A., Labhardt, L., Macchetto, F. D., Panagia, N. 1999, *ApJ*, 522, 802
- Sasselov, D. D., et al. 1997, *A&A*, 324, 471
- Schmidt K.-H., Priebe A., Boller T. 1993, *Astron. Nachr.* 314, 371
- Stanek, K. Z., Udalski, A. 1999, preprint (astro-ph/9909346)
- Stanek, K. Z., Kaluzny, J., Wysocka, A., & Thompson, I., 2000, *AcA*, 50, 191
- Stanek, K. Z. et al. 2001, in preparation
- Stephens, A. W. et al. 2000, preprint (astro-ph/0011045)
- Stetson, P. B. et al. 1998, *ApJ*, 508, 491
- Stetson, P. B. 1987, *PASP*, 99 191
- Stetson, P. B. 1992, in *ASP Conf. Ser. 25, Astrophysical Data Analysis Software and Systems I*, eds. D. M. Worrall, C. Bimesderfer, & J. Barnes (San Francisco: ASP), 297

Udalski, A., Soszyński, I., Szymański, M., Kubiak, M., Pietrzyński, G., Woźniak, P. & Żebruń, K.
1999, *Acta Astronomica*, 49, 223

Udalski, A., Szymański, M., Kubiak, M., Pietrzyński, G., Soszyński, I., Woźniak, P., Żebruń, K.
2000, *AcA*, 50, 307

Udalski, A. 2000, *ApJ*, 531L, 25

Table 4. THE K-S TEST RESULTS

Period	Σ_V	$P_{KS}^{C,U}$	$P_{KS}^{U,A}$	N_C
$P < 10^d$	> 21.6	100.0	0.9	21
	$20.8 \div 21.6$	99.5	93.0	13
$P > 10^d$	> 21.6	100.0	3.4	16
	$20.8 \div 21.6$	97.1	9.9	36
	< 20.8	92.9	31.0	8

Note. — C - the corrected Cepheid blending catalog (Tab. 1); U - the original uncorrected Cepheid blending catalog; A - the artificial Cepheid crowding catalog.

Table 1. THE M33 CEPHEID BLENDING CATALOG

Name	P	$\langle V \rangle$	$\langle I \rangle$	$\langle B \rangle$	N_V	S_V	N_I	S_I	N_B	S_B	σ_V
D33J013353.5+304744.1	4.31	21.17	...	21.55	5	0.91	4	1.24	22.00
D33J013359.4+304214.2	4.78	21.62	20.76	...	3	0.26	1	0.07	21.13
D33J013347.8+304627.4	4.86	20.83	...	21.38	0	0.00	0	0.00	21.82
D33J013357.0+304826.4	5.00	21.51	21.09	21.88	2	0.23	21.98
D33J013400.4+304808.8	5.10	21.23	20.28	21.99	6	1.18	22.12
D33J013408.6+303754.8	5.32	21.14	...	21.70	2	0.24	2	0.34	1	0.07	21.26
D33J013347.5+304456.2	5.35	99.00	...	20.60	2	0.41	21.16
D33J013421.6+304415.9	5.36	20.84	19.49	21.80	2	0.26	2	0.21	21.93
D33J013405.5+304133.3	5.38	21.86	...	22.43	0	0.00	2	0.24	21.18
D33J013357.0+303117.5	5.55	20.60	19.52	21.19	1	0.19	2	0.56	0	0.00	22.15
D33J013351.2+303001.0	5.60	20.50	19.57	21.15	1	0.10	1	0.24	22.13
D33J013350.0+304346.7	5.64	21.02	20.59	21.38	2	0.37	21.29
D33J013417.1+303932.9	5.64	19.88	19.41	20.26	3	0.94	21.88
D33J013420.6+304244.2	5.70	21.32	20.39	22.00	2	0.27	2	0.26	22.10
D33J013426.8+304357.7	5.70	19.83	19.46	...	2	0.25	1	0.21	22.13
D33J013350.6+304734.9	5.74	21.51	20.63	22.13	2	0.17	3	0.40	22.07
D33J013405.0+303557.5	5.89	21.14	20.45	21.62	2	0.20	21.36
D33J013407.9+303831.6	5.90	20.23	19.75	20.72	6	0.97	6	1.35	3	1.08	21.04
D33J013424.9+304431.2	5.91	21.29	20.09	22.31	4	0.80	0	0.00	21.88
D33J013346.9+304334.2	6.00	20.84	19.88	21.39	6	0.81	21.02
D33J013349.6+304744.7	6.00	21.82	20.39	...	1	0.21	1	0.30	22.17
D33J013350.6+303445.8	6.03	21.03	20.32	21.69	6	1.18	3	0.82	21.21
D33J013356.7+304838.6	6.12	20.90	20.09	21.32	1	0.07	21.94
D33J013349.4+303009.4	6.78	21.03	20.33	21.19	4	0.33	3	0.25	22.12
D33J013406.4+304003.7	6.93	20.47	19.48	21.06	2	0.20	2	0.29	20.89
D33J013428.3+303900.4	6.99	21.15	20.29	21.65	1	0.08	1	0.12	22.47
D33J013410.3+303934.8	7.09	21.39	20.88	21.98	1	0.07	21.28
D33J013422.5+304408.4	7.66	21.23	20.14	22.01	3	0.35	1	0.23	21.99
D33J013332.4+303143.3	7.97	21.40	20.22	22.59	1	0.35	0	0.00	21.87
D33J013348.8+303415.8	7.97	20.26	...	20.91	2	0.23	2	0.55	21.30
D33J013356.2+303909.1	8.57	20.51	19.26	...	3	0.71	4	1.27	3	0.97	20.39
D33J013406.6+303816.8	8.58	20.21	2	0.13	1	0.09	1	0.13	20.97
D33J013337.5+303305.1	8.98	20.97	19.99	...	2	0.19	2	0.32	21.41
D33J013333.5+303320.5	9.02	19.82	19.34	20.09	2	0.97	2	2.63	21.35
D33J013346.3+302908.9	9.12	20.51	19.76	20.90	2	0.21	3	0.21	22.23
D33J013352.7+303416.2	9.22	21.02	19.34	21.72	4	0.47	2	0.22	1	0.15	21.29
D33J013350.8+304715.5	9.72	20.73	20.02	21.42	0	0.00	0	0.00	22.04
D33J013421.1+304415.5	9.98	20.61	19.78	21.10	3	0.33	3	0.58	21.92
D33J013408.8+303946.5	10.11	20.47	19.42	21.07	1	0.08	3	0.72	21.12
D33J013355.0+303537.0	10.13	20.50	19.60	21.07	1	0.07	0	0.00	1	0.18	21.15

Table 1. CONTINUED.

Name	P	$\langle V \rangle$	$\langle I \rangle$	$\langle B \rangle$	N_V	S_V	N_I	S_I	N_B	S_B	σ_V
D33J013342.1+303210.7	10.38	21.01	19.14	...	2	0.17	2	0.50	21.40
D33J013356.1+303903.0	10.42	20.43	2	0.18	5	0.54	0	0.00	20.41
D33J013335.6+303649.2	10.70	20.73	20.24	22.10	1	0.07	1	0.09	21.22
D33J013327.4+303550.9	11.21	20.49	19.79	21.33	2	0.16	2	0.21	1	0.14	21.64
D33J013325.7+303426.6	11.45	20.19	19.47	20.82	0	0.00	0	0.00	21.93
D33J013353.4+303308.5	11.48	21.38	20.63	...	2	0.13	1	0.08	0	0.00	21.48
D33J013335.5+303330.2	11.52	20.55	19.69	21.36	1	0.14	1	0.24	21.40
D33J013357.4+304113.9	11.62	20.25	19.23	20.78	3	1.39	4	1.35	20.94
D33J013337.7+303218.9	11.88	20.80	19.74	...	0	0.00	0	0.00	21.40
D33J013420.3+304351.9	11.97	20.33	19.43	21.08	1	0.10	1	0.14	21.97
D33J013357.6+303805.4	12.34	20.48	19.71	...	1	0.16	1	0.08	20.92
D33J013351.1+304400.4	12.35	21.06	20.05	22.01	0	0.00	21.39
D33J013346.6+304821.8	12.36	20.13	18.38	21.28	1	0.07	1	0.08	21.97
D33J013256.3+303437.1	12.82	20.57	19.72	...	0	0.00	0	0.00	22.66
D33J013349.8+303758.7	12.91	20.16	19.74	...	1	0.06	2	0.20	20.70
D33J013350.0+303014.9	12.98	20.64	19.32	21.41	1	0.07	2	0.48	22.09
D33J013402.8+304145.7	13.04	19.93	18.80	20.60	2	0.18	4	0.75	21.13
D33J013345.9+304421.4	13.12	20.48	...	21.51	1	0.42	21.22
D33J013331.7+303931.1	13.17	20.13	19.37	20.79	2	0.19	1	0.14	1	0.32	21.55
D33J013325.5+304037.5	13.30	20.25	19.30	21.38	1	0.06	1	0.06	21.86
D33J013408.1+303931.9	13.32	20.32	19.73	20.55	5	0.78	3	0.38	21.07
D33J013351.2+303758.2	13.56	19.80	0	0.00	0	0.00	20.56
D33J013402.5+303628.0	13.65	20.36	19.43	20.77	3	0.39	20.93
D33J013408.4+303817.2	14.35	20.17	19.14	...	2	0.36	2	0.39	2	0.85	21.14
D33J013405.9+303928.9	14.60	19.92	19.21	...	2	0.38	2	0.25	20.90
D33J013327.8+303423.2	14.85	19.51	18.81	19.93	2	0.15	1	0.10	21.86
D33J013401.3+304026.9	14.85	19.86	19.26	20.17	4	1.48	4	0.70	20.84
D33J013334.4+303530.2	15.84	19.76	18.82	20.24	2	0.32	2	0.20	3	0.89	21.20
D33J013403.9+303615.8	16.28	20.26	19.22	21.00	0	0.00	21.09
D33J013353.4+303535.3	17.48	19.68	18.94	...	1	0.11	1	0.17	21.05
D33J013330.2+303637.4	17.98	20.17	18.94	20.61	0	0.00	0	0.00	1	0.08	21.37
D33J013346.6+304645.9	18.82	19.70	18.84	20.60	0	0.00	0	0.00	21.88
D33J013406.8+303940.2	18.89	19.76	18.86	20.51	5	0.46	4	0.34	20.91
D33J013330.2+303803.7	19.92	19.99	19.19	20.59	2	0.39	2	0.16	2	0.28	21.50
D33J013326.2+303319.4	19.99	20.16	19.19	21.03	0	0.00	0	0.00	22.01
D33J013331.5+303351.2	20.17	19.09	...	20.49	0	0.00	0	0.00	21.46
D33J013343.4+304356.5	20.19	19.33	18.83	19.51	4	1.70	21.40
D33J013419.0+304441.4	20.21	20.17	18.79	21.27	2	0.24	0	0.00	21.74
D33J013255.6+303512.9	21.06	20.02	19.16	20.99	0	0.00	0	0.00	22.57
D33J013401.7+303923.1	21.68	19.81	18.74	...	1	0.08	0	0.00	3	0.53	20.84

Table 1. CONTINUED.

Name	P	$\langle V \rangle$	$\langle I \rangle$	$\langle B \rangle$	N_V	S_V	N_I	S_I	N_B	S_B	σ_V
D33J013351.4+303830.7	21.79	20.20	18.87	...	1	0.10	4	0.73	0	0.00	20.32
D33J013330.4+303555.0	22.09	19.35	18.66	20.28	0	0.00	0	0.00	0	0.00	21.41
D33J013333.3+303747.1	22.68	20.51	19.30	...	0	0.00	1	0.40	0	0.00	21.43
D33J013417.6+303819.7	23.30	20.22	19.14	21.12	1	0.11	0	0.00	21.66
D33J013350.7+303544.2	23.31	19.88	18.89	...	0	0.00	1	0.06	21.23
D33J013358.8+303719.7	24.56	20.01	18.81	...	1	0.06	21.14
D33J013350.6+304754.7	26.48	19.93	18.62	21.10	1	0.11	1	0.36	22.21
D33J013354.3+304111.2	27.98	19.08	...	19.92	2	0.15	1	0.10	20.83
D33J013332.9+303548.4	30.29	19.44	18.50	...	3	0.22	3	0.29	3	0.40	21.15
D33J013302.3+303632.9	30.53	19.52	18.65	20.44	0	0.00	22.78
D33J013329.5+303556.9	30.66	19.58	18.65	20.55	1	0.10	1	0.06	1	0.15	21.43
D33J013354.8+304106.5	33.95	19.14	18.11	20.00	1	0.07	2	0.28	2	0.22	20.79
D33J013352.4+303844.2	35.94	19.11	18.10	...	0	0.00	1	0.10	0	0.00	20.20
D33J013327.5+303707.2	37.28	19.11	18.15	20.05	0	0.00	0	0.00	0	0.00	21.50
D33J013350.9+303336.1	37.57	20.48	19.03	21.74	0	0.00	0	0.00	21.40
D33J013329.3+303744.4	46.01	19.10	18.07	20.36	0	0.00	0	0.00	0	0.00	21.47
D33J013359.4+303226.7	50.28	19.87	18.45	20.82	0	0.00	21.75
D33J013347.5+304423.2	55.98	19.46	18.28	20.71	0	0.00	21.12
D33J013403.8+303911.1	57.44	19.56	18.21	20.64	0	0.00	0	0.00	1	0.20	20.90
D33J013337.5+303138.5	57.63	19.17	18.03	...	1	0.07	1	0.36	21.48
D33J013351.3+303900.9	62.00	17.44	0	0.00	0	0.00	2	0.15	19.85
D33J013351.8+303951.0	67.32	18.32	17.54	...	0	0.00	1	0.07	1	0.10	19.73